



Potent antiviral activity of novel multi-substituted 4-anilinoquin(az)olines

Sirle Saul^a, Szu-Yuan Pu^a, William J. Zuercher^{b,c}, Shirit Einav^{a,*}, Christopher R.M. Asquith^{b,d,*}

^a Department of Medicine, Division of Infectious Diseases and Geographic Medicine, and Department of Microbiology and Immunology, Stanford University School of Medicine, Stanford, CA 94305, USA

^b Structural Genomics Consortium, UNC Eshelman School of Pharmacy, University of North Carolina at Chapel Hill, Chapel Hill, NC 27599, USA

^c Lineberger Comprehensive Cancer Center, University of North Carolina at Chapel Hill, Chapel Hill, NC 27599, USA

^d Department of Pharmacology, School of Medicine, University of North Carolina at Chapel Hill, Chapel Hill, NC 27599, USA

ARTICLE INFO

Keywords:

Dengue Virus
Flavivirus
4-Anilinoquinoline
4-Anilinoquinazoline
Antiviral

ABSTRACT

Screening a series of 4-anilinoquinolines and 4-anilinoquinazolines enabled identification of potent novel inhibitors of dengue virus (DENV). Preparation of focused 4-anilinoquinoline/quinazoline scaffold arrays led to the identification of a series of high potency 6-substituted bromine and iodine derivatives. The most potent compound 6-iodo-4-((3,4,5-trimethoxyphenyl)amino)quinoline-3-carbonitrile (**47**) inhibited DENV infection with an EC₅₀ = 79 nM. Crucially, these compounds showed very limited toxicity with CC₅₀ values > 10 μM in almost all cases. This new promising series provides an anchor point for further development to optimize compound properties.

In the past five decades there has been a dramatic increase in the global burden of the mosquito-borne dengue virus (DENV) infection. The geographical range of dengue infections, including those in the developed world, has been expanding due to climate change and rapid urbanization.¹ Consequently, ~400 million people are estimated to get infected with one or more of the 4 distinct DENV serotypes annually in over 128 endemic countries.^{2,3} The majority of symptomatic individuals experience an uncomplicated dengue fever infection. However, 5–20% progress to a life-threatening disease, known as severe dengue, particularly upon a secondary infection with a heterologous DENV serotype.^{4,5}

The development of an effective dengue vaccine has been hampered by the necessity to generate simultaneous protection against the 4 distinct DENV serotypes.^{6,7} Moreover, since there are no approved antiviral therapies currently available, the management of dengue infections remains focused on the treatment of symptoms, rather than the underlying disease.⁸ This results in continued morbidity and mortality.

In recent years, there has been a flurry of activity to identify novel DENV inhibitors,^{9–24} but none of these compounds have yet entered clinical trials. These compounds include a number of kinase inhibitor scaffolds, such as the oxindole (sunitinib, JMX0395),^{9,10} azaindole (**1**)¹¹ and isothiazolo[4,3-*b*]pyridine (**2–3**)^{12,13} (Fig. 1).

To identify new chemical starting points to inhibit DENV, we looked to the chemically tractable 4-anilinoquin(az)oline scaffold. Our team

recently reported erlotinib as a promising starting point with activity against DENV replication (Fig. 2).⁹ There are a number of other quin(az)oline based inhibitors that have shown potent anti-DENV activity in the low nanomolar range, including RYL-634, **4** and **5** among others (Fig. 2).^{9,22–26} These results focused our attention on exploring the possible anti-DENV activity of the quin(az)oline scaffold.

To further explore antiviral quin(az)oline activity, we probed the structure activity relationships (SAR) of the quinoline/quinazoline by profiling several focused arrays of compounds. We developed a series of hybrid molecules combining structural features of erlotinib and **2** to expand the SAR in the current literature and assess tractability of the scaffolds (Fig. 3).

We hence synthesized a series of compounds (**6–64**) to follow up on the initial results of erlotinib and **2** to explore the 4-anilinoquinazoline and 4-anilinoquinoline scaffolds through nucleophilic aromatic displacement of 4-chloroquin(az)olines (Scheme 1).^{27–36} We were able to access products in good to excellent yields (34–83%) consistent with previous reports for literature and novel compounds.^{27–37}

We tested the compounds for antiviral activity in human hepatoma (Huh7) cells infected with DENV2.^{38–41} Their effect on overall infection was measured at 48 h post-infection via luciferase assays and the half-maximal effective concentration and the 90% effective concentrations (EC₅₀ and EC₉₀ values, respectively) were calculated. In parallel, we tested the effect of these compounds on cell viability via an AlamarBlue

* Corresponding authors at: Department of Medicine, Division of Infectious Diseases and Geographic Medicine, and Department of Microbiology and Immunology, Stanford University School of Medicine, Stanford, CA 94305, USA (S. Einav) and Department of Pharmacology, School of Medicine, University of North Carolina at Chapel Hill, Chapel Hill, NC 27599, USA (C.R.M. Asquith).

E-mail addresses: seinav@stanford.edu (S. Einav), chris.asquith@unc.edu (C.R.M. Asquith).

<https://doi.org/10.1016/j.bmcl.2020.127284>

Received 1 May 2020; Received in revised form 19 May 2020; Accepted 20 May 2020

Available online 27 May 2020

0960-894X/ © 2020 Elsevier Ltd. All rights reserved.

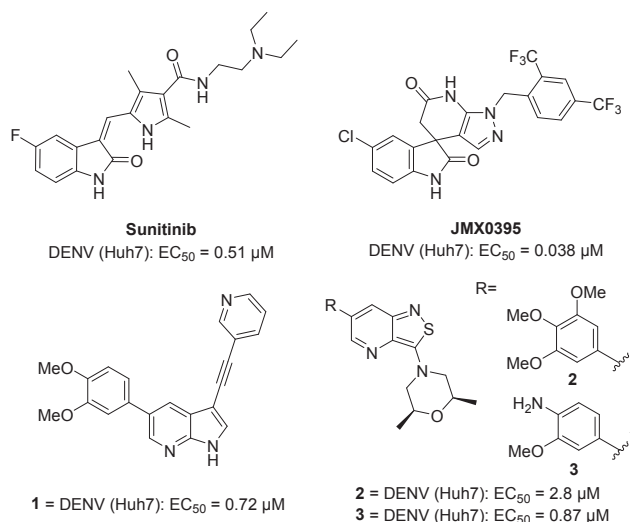


Fig. 1. A selection of previously reported inhibitors and associated activities on DENV (the data is all for serotype 2 for consistency). Huh7 = human hepatoma cells.

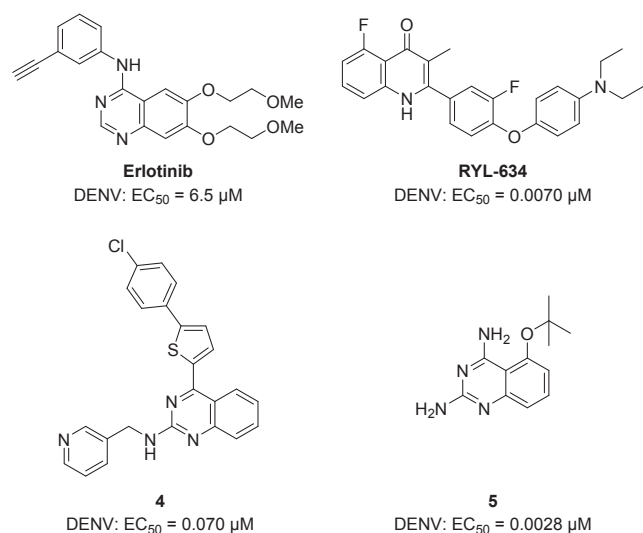


Fig. 2. Structures of quinazolines with anti-DENV activity.

assay in the DENV-infected Huh7 cells and measured the half-maximal cytotoxic concentration (CC_{50}) values.⁴²

We first screened a series of trimethoxyanilinoquinazolines (**6–24**) (Table 1).³² The unsubstituted trimethoxyanilinoquinazoline (**6**) showed a 2-fold increase in potency over erlotinib. However, further simple substitutions with a 6-methyl (**7**), 6-fluoro (**8**) or 6,7-difluoro (**9**) showed no activity or toxicity. Interestingly, the switch from 6-fluoro (**9**) to 6-chloro (**10**) led to a > 10-fold increase in activity and an almost 7-fold increase with respect to erlotinib. Similar activity values were observed for compounds possessing 6-bromo (**11**) and 6-iodo (**12**). However, when there was an increase in size and electronegativity to 6-trifluoromethyl (**13**) the compound was inactive. Switching the halogen to the 7-position (**14–18**) led to net decrease in activity. The 7-fluoro (**14**) was inactive and the 7-chloro (**15**) was equivalent to erlotinib and 6-fold less potent than the 6-chloro counterpart (**10**). The 7-bromo (**16**) and 7-iodo (**17**) were only 2- and 3-fold less potent respectively. In contrast, the 7-trifluoromethyl (**18**) was more active than **13**, its regioisomer at the 6-position, with equivalent activity to erlotinib. The 7-cyano (**19**) saw an increase in potency to almost 5-fold more than erlotinib with an $EC_{50} = 1.4 \mu M$. The 6-cyano (**20**) was 2-fold weaker,

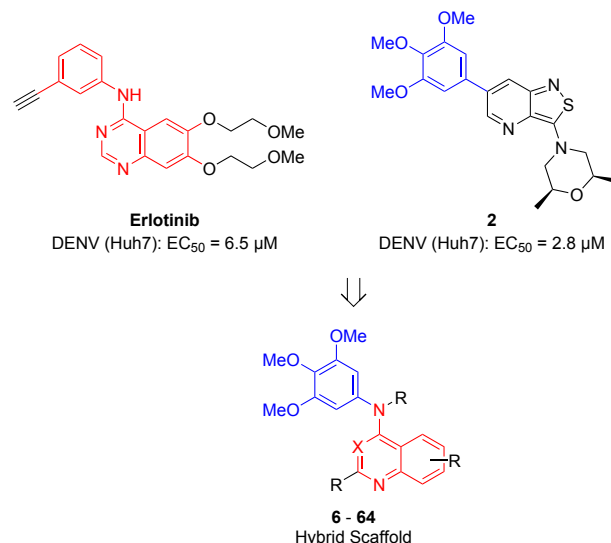


Fig. 3. Depiction of a hybrid series of trimethoxyanilinoquin(az)olines developed by combining erlotinib and **2**.

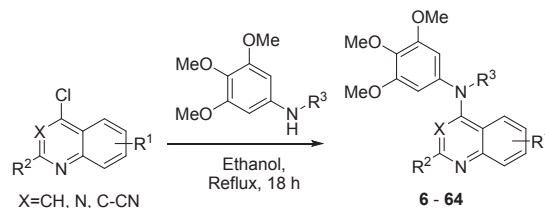


Table 1

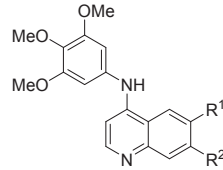
Screening results of SAR of trimethoxy quinazolines and anti-DENV activity.

Cmpd	R ¹	R ²	DENV inhibition	
			EC_{50}^a (μM)	CC_{50}^b (μM)
6	H	H	2.8	> 10
7	Me	H	> 10	> 10
8	F	H	> 10	> 10
9	F	F	> 10	> 10
10	Cl	H	1.0	> 10
11	Br	H	0.97	> 10
12	I	H	1.0	> 10
13	CF ₃	H	> 10	> 10
14	H	F	> 10	> 10
15	H	Cl	6.1	> 10
16	H	Br	2.0	> 10
17	H	I	2.9	5.8
18	H	CF ₃	5.1	> 10
19	H	CN	1.4	> 10
20	CN	H	3.7	> 10
21	SO ₂ Me	H	> 10	> 10
22	OMe	H	> 10	> 10
23	OMe	OMe	6.6	> 10
24	H	OMe	2.7	> 10

a = infectivity assay in Huh7 cells mean average n = 2; b = cytotoxicity in Huh7 cells mean average n = 2.

Table 2

Screening results of SAR of trimethoxy quinolines and anti-DENV activity.



The chemical structure shows a quinoline core. At position 2, there is an amino group (-NH-) connected to a benzene ring. This benzene ring has methoxy (-OMe) groups at positions 3, 4, and 5. The quinoline core has substituents R¹ at position 6 and R² at position 7.

Compd	R ¹	R ²	DENV inhibition	
			EC ₅₀ ^a (μM)	CC ₅₀ ^b (μM)
25	H	H	0.82	> 10
26	F	H	0.52	> 10
27	F	F	1.0	5.5
28	Cl	H	0.52	> 10
29	Br	H	0.080	> 10
30	I	H	0.82	> 10
31	CF ₃	H	0.59	> 10
32	CN	H	0.76	> 10
33	SO ₂ Me	H	0.84	> 10
34	^t Bu	H	7.4	> 10
35	OMe	H	0.75	> 10
36	OMe	OMe	> 10	> 10
37	H	OMe	> 10	> 10
38	H	F	4.1	> 10
39	H	Cl	> 10	> 10
40	H	Br	8.4	> 10
41	H	I	3.6	> 10
42	H	CF ₃	6.8	> 10
43	H	CN	3.3	> 10

a = infectivity assay in Huh7 cells mean average n = 2; b = cytotoxicity in Huh7 cells mean average n = 2.

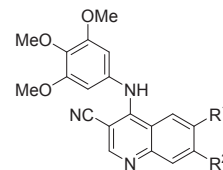
while the 6-methylsulfone (21) was inactive as was the corresponding 6-methoxy substitution (22). The 6,7-dimethoxy analog (23) had equivalent potency to erlotinib. Interestingly the 7-methoxy analog (24) showed a 2-fold increase in activity relative to erlotinib and 23.

Even small changes to the central plane angle can have radical effects on the scaffold's biological properties. Consequently, we hypothesized that switching from the quinazoline to the quinoline core would more closely mimic the central plane angle present in **1** and lead to more potent activity. The change from quinoline to quinazoline was expected to increase the plane angle from nearly planar to around 50–60 degrees.³² Our hypothesis proved to be valid as the unsubstituted trimethoxyanilinoquinoline (25) was 3-fold more potent than the corresponding quinoline (6) and 8-fold more potent than erlotinib (Table 2). The 6-fluoro analog (26) had equivalent potency to 25. The 6,7-difluoro (27) was also equivalent but showed toxicity at higher concentrations (CC₅₀ = 5.5 μM). The 6-chloro analog (28) was equivalent to the 6-fluoro (26), and the 6-bromo (29) exhibited a substantial increase in potency (EC₅₀ = 80 nM), with a > 80-fold increase over erlotinib and 10-fold over the unsubstituted analog (25). The 6-bromo analog (29) demonstrated a local activity minimum as further substitution to increase the halogen size to 6-iodo (30) and 6-trifluoromethyl (31), along with the corresponding 6-cyano (32) and methylsulfone (33) all showed potency in the range 0.5–1 μM.

The incorporation of a slightly larger substituent, a 6-*tert*-butyl (34), led to an activity down to that of erlotinib. Switching to the 6-methoxy analog (35) recovered the potency loss with an almost 8-fold increase over erlotinib. Surprisingly, the 6,7-dimethoxy analog (36) showed no activity (n = 4 biological replicates) and neither did the 7-methoxy substitution (37). The other 7-position analogs (38–43) all demonstrated weaker activity. Variation of the halogen (38–42) resulted in no clear trend with the 7-iodo (41) the only compound with a 2-fold improvement over erlotinib. The 7-cyano (43) yielded equipotent activity to 41 with an EC₅₀ = 3.3 μM with an increased ligand efficiency.

Table 3

Screening results of SAR of trimethoxy 3-cyanoquinolines and anti-DENV activity.



The chemical structure shows a quinoline core. At position 2, there is an amino group (-NH-) connected to a benzene ring. This benzene ring has methoxy (-OMe) groups at positions 3, 4, and 5. At position 3 of the quinoline core, there is a cyano group (-NC). The quinoline core has substituents R¹ at position 6 and R² at position 7.

Compd	R ¹	R ²	DENV inhibition	
			EC ₅₀ ^a (μM)	CC ₅₀ ^b (μM)
44	H	H	> 10	> 10
45	Cl	H	1.3	> 10
46	Br	H	0.082	> 10
47	I	H	0.079	> 10
48	SO ₂ Me	H	> 10	> 10
49	OMe	H	3.1	> 10
50	OMe	OMe	5.5	> 10
51	H	OMe	> 10	> 10
52	H	Cl	> 10	> 10
53	H	Br	> 10	> 10
54	H	I	4.7	> 10

a = infectivity assay in Huh7 cells mean average n = 2; b = cytotoxicity in Huh7 cells mean average n = 2.

To increase the plane angle to near orthogonality, we switched to the 3-cyanoquinoline (44–54) (Table 3).³² The initial result was disappointing with the unsubstituted analog (44) having no observable activity up to the highest compound concentrations employed. Switching to the 6-chloro (45) yielded an analog with activity just above micromolar (EC₅₀ = 1.3 μM). However, the 6-bromo (46) and 6-iodo (47) had activities equivalent to 29 and with a > 80-fold increase over erlotinib and 120-fold over the unsubstituted analog. Switching to the 6-methylsulfone (48) removed all activity. Some recovery of activity to EC₅₀ = 3.3 μM was possible switching to the 6-methoxy (49). However, the 6,7-dimethoxy (50) showed a slight reduction in potency and the 7-methoxy (51) was inactive. Results were similar for the 7-chloro (52) and 7-bromo (53). Interestingly, there was some recovery with the 7-iodo (54) with an EC₅₀ = 4.7 μM.

We sought to further understand the observed SAR between the quinazoline scaffold and the DENV inhibition profiles. This was achieved by synthesizing a series of derivatives with different electronic and steric profiles (55–64) (Table 4).^{28,36} First, the direct 6-bromo analog (55) of 29 with a 2-methyl substitution was > 20-fold more potent than erlotinib but with an unexpected increase in toxicity (CC₅₀ = 2.5 μM) with only a 10-fold selectivity index (CC₅₀/EC₅₀). Switching to the 6-methoxy (56), 6,7-dimethoxy (57), 7-methoxy (58) all yielded analogs with limited or no activity in addition to no toxicity. The 7-trifluoromethyl (59) was also inactive. However, moving the trifluoromethyl to the 6-position (60) yielded a compound that was 3-fold less potent than the 6-bromo (55), but with no toxicity and 7-fold more potency than erlotinib. Moving the methyl group to block the amino bridge (61) removed all activity. Switching the trifluoromethyl for a simple fluorine (62) decreased potency by over 2-fold. The 2-methyl group (63) was weakly active and the 8-methyl substitution (64) was inactive. These two results taken together suggest that the quinoline nitrogen is an important contributor to activity.

These results delineate the SAR of anti-DENV activity and the 4-anilinoquinoline/quinazoline scaffold. The 6-position bromine and iodine analogs on the quinoline were by far the most potent series of analogs (29, 46, 47 and 55) (Fig. 4).

This body of work provides several exciting starting points for further optimization. The mechanism of the observed antiviral activity has

Table 4

Screening results of SAR of the trimethoxy quinoline core and anti-DENV activity.

Cmpd	R ¹	R ²	R ³	R ⁴	R ⁵	DENV inhibition	
						EC ₅₀ ^a (μM)	CC ₅₀ ^b (μM)
55	Br	H	Me	H	H	0.28	2.5
56	OMe	H	Me	H	H	10	> 10
57	OMe	OMe	Me	H	H	10	> 10
58	H	OMe	Me	H	H	> 10	> 10
59	H	CF ₃	Me	H	H	> 10	> 10
60	CF ₃	H	Me	H	H	0.91	> 10
61	CF ₃	H	H	Me	H	> 10	> 10
62	F	H	Me	H	H	2.3	> 10
63	H	H	Me	H	H	8.0	> 10
64	H	H	H	H	Me	> 10	> 10

a = infectivity assay in Huh7 cells mean average n = 2; b = cytotoxicity in Huh7 cells mean average n = 2.

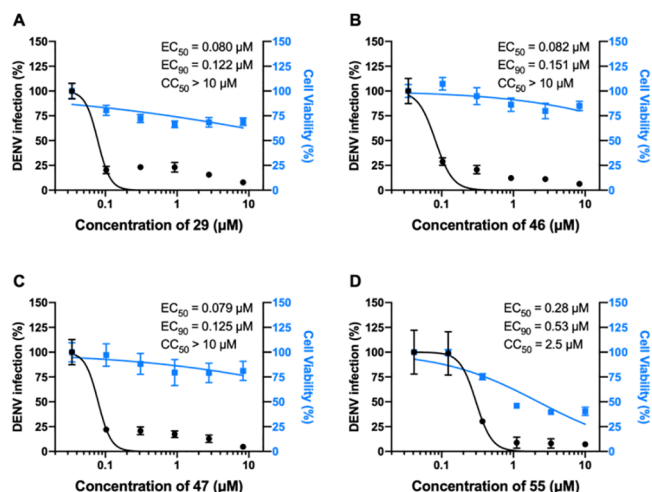


Fig. 4. Compounds **29**, **46**, **47** and **55** suppress DENV infection. Dose response of DENV infection (black) and cell viability (blue) to compounds **29** (A), **46** (B), **47** (C) and **55** (D) measured by luciferase and alamarBlue assays, respectively, 48 h after infection. Data are plotted relative to vehicle control. Shown are representative experiments from at least two conducted, each with 5 biological replicates; shown are means \pm SD.

yet to be defined and could be a combination of factors including kinases and other proteins. Some of these compounds are known to act as kinase inhibitors having been originally prepared as inhibitors targeting the ATP-binding site of human kinases including cyclin-G-associated kinase (GAK), serine/threonine-protein kinase 10 (STK10) and STE20-like serine/threonine-protein kinase (SLK).³² It is possible that these kinases may be involved, but their ATP-binding sites may not be directly involved. Alternatively, other undefined proteins may participate in the mechanism of antiviral action. Indeed, compounds having structural features expected to impede interaction with a kinase hinge region (Table 4) also demonstrated antiviral activity. It is also possible that the observed phenotypes may originate from modulation of other, non-kinase ATP or non-ATP binding proteins.⁴³ Lastly, we cannot

exclude a possibility that these compounds target a viral protein.

Erlotinib and **2** have both previously been reported to inhibit DENV replication.⁹ The synthetic combination of these two molecules to form a series of trimethoxyquin(az)olines has defined a new series of DENV inhibitors. Several key results act as a signpost for further chemical optimization. The 6,7-dimethoxy-*N*-(3,4,5-trimethoxyphenyl)quinolin-4-amine analog **23** had equivalent potency to erlotinib showing that the glycol ether side chains are less important for activity. The 6-bromo-*N*-(3,4,5-trimethoxyphenyl)quinolin-4-amine analog **29** demonstrated a local minimum in the SAR, highlighting that a medium sized group was optimal in this position. The 6-bromo (**46**) and 6-iodo (**47**) 3-cyanoquinoline compounds supported this with activities equivalent to **29** and a > 80-fold increase over erlotinib and 120-fold over the unsubstituted analog (**44**). This initial series of results are the first step in defining a medicinal chemistry trajectory towards a series of optimized antiviral compounds with potential to treat DENV and possibly other viral agents.

Declaration of Competing Interest

The authors declare that they have no known competing financial interests or personal relationships that could have appeared to influence the work reported in this paper.

Acknowledgments

This work was supported by award number W81XWH-16-1-0691 from the Department of Defense (DoD), Congressionally Directed Medical Research Programs (CDMRP) and HDTRA11810039 from the Defense Threat Reduction Agency (DTRA)/Fundamental Research to Counter Weapons of Mass Destruction to SE. The SGC is a registered charity (number 1097737) that receives funds from AbbVie, Bayer Pharma AG, Boehringer Ingelheim, Canada Foundation for Innovation, Eshelman Institute for Innovation, Genome Canada, Innovative Medicines Initiative (EU/EFPIA) [ULTRA-DD grant no. 115766], Janssen, Merck KGaA Darmstadt Germany, MSD, Novartis Pharma AG, Ontario Ministry of Economic Development and Innovation, Pfizer, São Paulo Research Foundation-FAPESP, Takeda, and Wellcome [106169/ZZ14/Z]. We are grateful Dr. Brandie Ehrmann and Miss Diane E. Wallace for LC-MS/HRMS support provided by the Mass Spectrometry Core Laboratory at the University of North Carolina at Chapel Hill. The opinions, interpretations, conclusions, and recommendations are those of the authors and are not necessarily endorsed by the U.S. Army or the other funders.

Appendix A. Supplementary data

Supplementary data to this article can be found online at <https://doi.org/10.1016/j.bmcl.2020.127284>.

References

- Messina JP, Brady OJ, Golding N, et al. *Nat Microbiol.* 2019;4:1508.
- Bhatt S, Gething PW, Brady OJ, et al. *Nature.* 2013;496:504.
- Guzman MG, Gubler DJ, Izquierdo A, Martinez E, Halstead SB. *Nat Rev Dis Primers.* 2016;18:16055.
- Machado CR, Machado ES, Rohloff RD, et al. *PLoS Negl Trop Dis.* 2013;7.
- Chau TN, Anders KL, Lien le B. *PLoS Negl Trop Dis.* 2010;4.
- Flipse J, Smit JM. *PLoS Negl Trop Dis.* 2015;9.
- Yang Y, Meng Y, Halloran M, E.; Longini, I. M. Jr. *Clin Infect Dis* 2018, 66, 178.
- Stevens AJ, Gahan ME, Mahalingam S, Keller PA. *J Med Chem.* 2009;52:7911.
- Bekerman E, Neveu G, Shulla A, et al. *J Clin Invest.* 2017;127:1338.
- Xu J, Xie X, Chen H, Zou J, et al. *Bioorg Med Chem Lett.* 2020;30.
- Verdonck S, Pu SY, Sorrell FJ, et al. *J Med Chem.* 2019;62:5810.
- Pu SY, Wouters R, Schor S, et al. *J Med Chem.* 2018;61:6178.
- Chen WC, Simanjuntak Y, Chu LW, et al. *J Med Chem.* 2020;63:1313.
- Bardot D.; Koukni, M.; Smets, W.; Carlens, G.; McNaughton, M.; Kaptein, S.; Dallmeier, K.; Chaltin, P. Neyts, J.; Marchand, A. *J Med Chem.* 2018, 61, 8390.
- Millies, B.; von Hammerstein, F.; Gellert, A.; Hammerschmidt, S.; Barthels, F.;

- Göppel, U.; Immerheiser, M.; Elgner, F.; Jung, N.; Basic, M.; Kersten, C.; Kiefer, W.; Bodem, J.; Hildt, E.; Windbergs, M.; Hellmich, U. A.; Schirmeister, T. *J Med Chem.* 2019, 62, 11359.
16. Vincetti P, Caporuscio F, Kaptein S, et al. *J Med Chem.* 2015;58:4964.
 17. Behnam MAM, Graf D, Bartenschlager R, Zlotos DP, Klein CD. *J Med Chem.* 2015;58:9354.
 18. Nitsche C, Steuer C, Klein CD. *Bioorg Med Chem.* 2011;19:7318.
 19. Saudi M, Zmurnko J, Kaptein S, Rozenski J, Neyts J, Van Aerschot A. *Eur J Med Chem.* 2014;87:529.
 20. Yokokawa F, Nilar S, Noble CG, et al. *J Med Chem.* 2016;59:3935.
 21. Yang CC, Hu HS, Wu RH, et al. *Antimicrob Agents Chemother.* 2014;58:110.
 22. Venkatesham A, Saudi M, Kaptein S, et al. *Eur J Med Chem.* 2017;126:101.
 23. Yang Y, Cao L, Gao H, et al. *J Med Chem.* 2019;62:4056.
 24. Wang QY, Patel SJ, Vangrevelinghe E, et al. *Antimicrob Agents Chemother.* 2019;63:1823.
 25. Chao B, Tong XK, Tang W, et al. *J Med Chem.* 2012;55:3135.
 26. Opsenica I, Burnett JC, Gussio R, et al. *J Med Chem.* 2011;54:1157.
 27. Asquith CRM, Laitinen T, Bennett JM, et al. *Chem Med Chem.* 2018;13:48.
 28. Asquith CRM, Berger BT, Wan J, et al. *J Med Chem.* 2019;62:2830.
 29. Asquith CRM, Naegeli KM, East MP, et al. *J Med Chem.* 2019;62:4772.
 30. Asquith CRM, Treiber DK, Zuercher WJ. *Bioorg Med Chem Lett.* 2019;29:1727.
 31. Asquith CRM, Bennett JM, Su L, et al. *Molecules.* 2019;24:p11 E4016.
 32. Asquith CRM, Laitinen T, Bennett JM, et al. *ChemMedChem.* 2020;15:26.
 33. Asquith CRM, Fleck N, Torrice CD. *Bioorg Med Chem Lett.* 2019;18:2695.
 34. Asquith CRM, Maffuid KA, Laitinen T, et al. *ChemMedChem.* 2019;14:1693.
 35. Asquith CRM, Tizzard G. *Molbank.* 2019;4:M1087.
 36. Asquith, C. R. M.; Laitinen, T.; Wells, C. I.; Tizzard, G. J.; Zuercher, W. J. *Molecules.* 2020, 25, pii: E1697.
 37. General procedure for the synthesis of 4-anilinoquin(az)olines: 4-chloroquin(az)oline derivative (1.0 eq.), aniline derivative (1.1 eq.), were suspended in ethanol (10 mL) and refluxed for 18 h. The crude mixture was purified by flash chromatography using EtOAc:hexane followed by 1-5 % methanol in EtOAc; After solvent removal under reduced pressure, the product was obtained as a free following solid or recrystallized from ethanol/water. Compounds 6-54 were synthesized as previous described³² and 60-61 as previously reported.²⁸ 6-bromo-2-methyl-N-(3,4,5-trimethoxyphenyl)quinolin-4-amine (55) was obtained as a light yellow solid (149 mg, 0.370 mmol, 63%). m.p. > 250 °C; ¹H NMR (400 MHz, DMSO-d₆) δ 10.87 – 10.61 (m, 1H), 9.06 (d, J = 2.0 Hz, 1H), 8.28 – 7.87 (m, 2H), 6.82, (s, 1H), 6.78 (s, 2H), 3.80 (s, 6H), 3.72 (s, 3H), 2.63 (s, 3H). ¹³C NMR (100 MHz, DMSO-d₆) δ 155.1, 153.6, 153.3, 137.6, 136.4, 136.1, 132.7 (s, 2C), 125.8, 122.1, 119.1, 117.6, 103.0 (s, 2C), 101.0, 60.2, 56.1 (s, 2C), 19.2. HRMS m/z [M+H]⁺ calcd for C₁₉H₂₀BrN₂O₃: 403.0657, found 403.0662, LC tR = 4.00 min, > 98% Purity. 6-methoxy-2-methyl-N-(3,4,5-trimethoxyphenyl)quinolin-4-amine (56) was obtained as a yellow solid (213 mg, 0.601 mmol, 83%). m.p. 135–137 °C; ¹H NMR (400 MHz, DMSO-d₆) δ 10.68 (s, 1H), 8.22 (d, J = 2.6 Hz, 1H), 8.05 (d, J = 9.2 Hz, 1H), 7.59 (dd, J = 9.2, 2.5 Hz, 1H), 6.80 (s, 2H), 6.74 (s, 1H), 3.98 (s, 3H), 3.81 (s, 6H), 3.72 (s, 3H), 2.61 (s, 3H). ¹³C NMR (100 MHz, DMSO-d₆) δ 157.5, 153.5, 153.4, 152.2, 136.2, 133.5, 133.1 (s, 2C), 124.7, 121.3, 117.3, 103.2 (s, 2C), 103.0, 100.1, 60.2, 56.5, 56.1 (s, 2C), 19.5. HRMS m/z [M+H]⁺ calcd for C₂₀H₂₃N₂O₄: 355.1658, found 355.1655, LC tR = 3.84 min, > 98% Purity. 6,7-dimethoxy-2-methyl-N-(3,4,5-trimethoxyphenyl)quinolin-4-amine (57) was obtained as a light yellow solid (187 mg, 0.483 mmol, 72%). m.p. > 250 °C; ¹H NMR (400 MHz, DMSO-d₆) δ 10.49 (s, 1H), 8.11 (s, 1H), 7.48 (s, 1H), 6.77 (s, 2H), 6.65 (s, 1H), 3.98 (s, 3H), 3.94 (s, 3H), 3.81 (s, 6H), 3.72 (s, 3H), 2.57 (s, 3H). ¹³C NMR (100 MHz, DMSO-d₆) δ 154.2, 153.5, 152.9, 151.2, 148.8, 136.1, 135.3, 133.2 (s, 2C), 110.2, 103.2 (s, 2C), 102.7, 99.6, 99.4, 60.2, 56.7, 56.1 (s, 2C), 56.0, 19.4. HRMS m/z [M+H]⁺ calcd for C₂₁H₂₅N₂O₅: 385.1763, found 385.1762, LC tR = 3.82 min, > 98% Purity. 7-methoxy-2-methyl-N-(3,4,5-trimethoxyphenyl)quinolin-4-amine (58) was obtained as a colourless solid (194 mg, 0.504 mmol, 80%). m.p. > 350 °C; ¹H NMR (400 MHz, DMSO-d₆) δ 10.63 (s, 1H), 8.67 (d, J = 9.3 Hz, 1H), 7.48 (d, J = 2.5 Hz, 1H), 7.35 (dd, J = 9.3, 2.5 Hz, 1H), 6.77 (s, 2H), 6.65 (s, 1H), 3.94 (s, 3H), 3.80 (s, 6H), 3.72 (s, 3H), 2.59 (s, 3H). ¹³C NMR (100 MHz, DMSO-d₆) δ 162.8, 154.1, 153.9, 153.5 (s, 2C), 140.8, 136.3, 133.0, 125.3, 117.2, 110.3, 103.3 (s, 2C), 99.8, 99.4, 60.2, 56.1 (s, 2C), 55.9, 19.6. HRMS m/z [M+H]⁺ calcd for C₂₀H₂₃N₂O₄: 355.1658, found 355.1639, LC tR = 3.18 min, > 98% Purity. 2-methyl-7-(trifluoromethyl)-N-(3,4,5-trimethoxyphenyl)quinolin-4-amine (59) was obtained as a yellow solid (165 mg, 0.421 mmol, 69%). m.p. > 250 °C; ¹H NMR (400 MHz, DMSO-d₆) δ 11.01 (s, 1H), 9.01 (d, J = 8.8 Hz, 1H), 8.53 (d, J = 1.9 Hz, 1H), 8.06 (dd, J = 9.0, 1.8 Hz, 1H), 6.89 (s, 1H), 6.81 (s, 2H), 3.81 (s, 6H), 3.73 (s, 3H), 2.67 (s, 3H). ¹³C NMR (100 MHz, DMSO-d₆) δ 155.1 (d, J = 212.2 Hz), 153.6 (s, 2C), 138.2, 136.5, 132.6, 132.5 (q, J = 32.2 Hz), 132.0, 125.7, 124.6, 122.0 – 121.6 (m), 118.4, 117.5 – 116.9 (m), 103.1 (s, 2C), 101.7, 60.2, 56.1 (s, 2C), 19.9. HRMS m/z [M+H]⁺ calcd for C₂₀H₂₀F₃N₂O₃: 393.1426, found 393.1422, LC tR = 4.07 min, > 98% Purity. 6-fluoro-2-methyl-N-(3,4,5-trimethoxyphenyl)quinolin-4-amine (62) was obtained as a light yellow solid (179 mg, 0.523 mmol, 68%). m.p. > 250 °C; ¹H NMR (400 MHz, DMSO-d₆) δ 10.72 (s, 1H), 8.71 (dd, J = 10.5, 2.7 Hz, 1H), 8.21 (dd, J = 9.3, 5.1 Hz, 1H), 7.92 (ddd, J = 9.3, 8.0, 2.7 Hz, 1H), 6.80 (d, J = 6.2 Hz, 3H), 3.80 (s, 6H), 3.72 (s, 3H), 2.64 (s, 3H). ¹³C NMR (100 MHz, DMSO-d₆) δ 159.5 (d, J = 244.9 Hz), 154.5, 153.9 (d, J = 3.8 Hz), 153.6 (s, 2C), 136.4, 135.6, 132.8, 122.8 (d, J = 17.2 Hz), 122.6, 117.2 (d, J = 9.5 Hz), 108.3 (d, J = 25.1 Hz), 103.1 (s, 2C), 100.4, 60.2, 56.1 (s, 2C), 19.7. HRMS m/z [M+H]⁺ calcd for C₁₉H₂₀FN₂O₃: 343.1458, found 343.1456, LC tR = 3.67 min, > 98% Purity. 2-methyl-N-(3,4,5-trimethoxyphenyl)quinolin-4-amine (63) was obtained as a colourless solid (200 mg, 0.616 mmol, 73%). m.p. > 250 °C; ¹H NMR (400 MHz, DMSO-d₆) δ 10.76 (s, 1H), 8.77 (dd, J = 8.6, 1.3 Hz, 1H), 8.11 (dd, J = 8.5, 1.2 Hz, 1H), 7.97 (ddd, J = 8.4, 7.0, 1.1 Hz, 1H), 7.72 (ddd, J = 8.3, 7.0, 1.2 Hz, 1H), 6.80 (s, 2H), 6.77 (s, 1H), 3.81 (s, 6H), 3.73 (s, 3H), 2.64 (s, 3H). ¹³C NMR (100 MHz, DMSO-d₆) δ 154.6, 154.4, 153.6 (s, 2C), 138.5, 136.4, 133.5, 132.9, 126.4, 123.4, 119.8, 116.1, 103.2 (s, 2C), 100.3, 60.2, 56.1 (s, 2C), 19.8. HRMS m/z [M+H]⁺ calcd for C₁₉H₂₁N₂O₃: 325.1552, found 325.1551, LC tR = 3.59 min, > 98% Purity. 8-methyl-N-(3,4,5-trimethoxyphenyl)quinolin-4-amine (64) was obtained as a mustard solid (93.1 mg, 0.287 mmol, 34%). m.p. 130–132 °C; ¹H NMR (400 MHz, DMSO-d₆) δ 13.45 (s, 1H), 10.77 (s, 1H), 8.56 (d, J = 8.5 Hz, 1H), 8.39 (d, J = 6.9 Hz, 1H), 7.86 (d, J = 7.1 Hz, 1H), 7.68 (dd, J = 8.5, 7.1 Hz, 1H), 6.90 (d, J = 6.8 Hz, 1H), 6.80 (s, 2H), 3.75 (d, J = 31.4 Hz, 9H), 2.68 (s, 3H). ¹³C NMR (100 MHz, DMSO-d₆) δ 155.4, 155.2, 153.7 (s, 2C), 136.5, 134.3, 134.2, 133.0, 126.6, 121.1, 117.2, 112.9, 103.2 (s, 2C), 100.6, 60.2, 56.2 (2, 2C), 17.8. HRMS m/z [M+H]⁺ calcd for C₁₉H₂₁N₂O₃: 325.1552, found 325.1550, LC tR = 3.60 min, > 98% Purity.
 38. Virus construct. DENV2 (New Guinea C strain)^{44,45} Renilla reporter plasmid used for in vitro assays was a gift from Pei-Yong Shi (The University of Texas Medical Branch).
 39. Cells. Huh7 (Apath LLC) cells were grown in DMEM (Mediatech) supplemented with 10% FBS (Omega Scientific), nonessential amino acids, 1% L-glutamine, and 1% penicillin-streptomycin (ThermoFisher Scientific) and maintained in a humidified incubator with 5% CO₂ at 37 °C.
 40. Virus Production. DENV2 RNA was transcribed in vitro using mMessage/mMachine (Ambion) kits. DENV was produced by electroporating RNA into BHK-21 cells, harvesting supernatants on day 10 and titrating via standard plaque assays on BHK-21 cells. In parallel, on day 2 post-electroporation, DENV-containing supernatant was used to inoculate C6/36 cells to amplify the virus.
 41. Infection assays. Huh7 cells were infected with DENV in replicates (n = 5) at a multiplicity of infection (MOI) of 0.05. Overall infection was measured at 48 hours using a Renilla luciferase substrate.
 42. Viability assays. Viability was assessed using AlamarBlue® reagent (Invitrogen) assay according to manufacturer's protocol. Fluorescence was detected at 560 nm on InfiniteM1000 plate reader.
 43. Munoz L. *Nat Rev Drug Discov.* 2017;16:424.
 44. Xie X, Gayen S, Kang C, Yuan Z, Shi P-Y. *J Virol.* 2013;87:4609.
 45. Zou G, Xu HY, Qing M, Wang QY, Shi PY. *Antiviral Res.* 2011;91:11.